

## Model predictive control strategies for protection of structures during earthquakes

Long-He Xu\*<sup>1</sup> and Zhong-Xian Li<sup>2a</sup>

<sup>1</sup>School of Civil Engineering, Beijing Jiaotong University, Beijing 100044, China

<sup>2</sup>School of Civil Engineering, Tianjin University, Tianjin 300072, China

(Received November 19, 2010, Revised June 25, 2011, Accepted August 17, 2011)

**Abstract.** This paper presents a theoretical study of a model predictive control (MPC) strategy employed in semi-active control system with magnetorheological (MR) dampers to reduce the responses of seismically excited structures. The MPC scheme is based on a prediction model of the system response to obtain the control actions by minimizing an objective function, which can compensate for the effect of time delay that occurred in real application. As an example, a 5-story building frame equipped with two 20 kN MR dampers is presented to demonstrate the performance of the proposed MPC scheme for addressing time delay and reducing the structural responses under different earthquakes, in which the predictive length  $l=5$  and the delayed time step  $d=10, 20, 40, 60, 100$  are considered. Comparison with passive-off, passive-on, and linear quadratic Gaussian (LQG) control strategy indicates that MPC scheme exhibits good control performance similar to the LQG control strategy, both have better control effectiveness than two passive control methods for most cases, and the MPC scheme used in semi-active control system show more effectiveness and robustness for addressing time delay and protecting structures during earthquakes.

**Keywords:** predictive control; semi-active control; magnetorheological dampers; earthquakes; time delay

---

### 1. Introduction

Earthquakes have always been a major nature disaster to society, as the Wenchuan earthquake in China and the recent East-Japan earthquake, have brought great losses to human life and economy primarily due to the collapse of structures. One of effective and practical methods to protect structures from damage due to strong wind and earthquakes is the structural control technique. Among these control methods, semi-active control technique has received much attention and has demonstrated a great deal of promise for civil engineering applications. Especially, the occurrence of some smart materials and controllable dampers, such as magnetorheological (MR) dampers, which combine the best features of active and passive devices, have the potential to improve the seismic behavior of full scale engineering structures, make the semi-active control technique more practical and feasible. Many analytical and experimental studies have been performed on their

---

\*Corresponding author, Associate Professor, E-mail: [lhxu@bjtu.edu.cn](mailto:lhxu@bjtu.edu.cn)

<sup>a</sup>Professor

behavior and applications to civil structures, and have shown better control performance in reducing seismic responses (Spencer *et al.* 1997a, b, Dyke *et al.* 1996, Carlson *et al.* 1996a, b, Hiemenz *et al.* 2003, Li and Xu 2005, Yang *et al.* 2004, Chang *et al.* 1999, Schurter and Roschke 2000).

Various control strategies have been evaluated and compared for semi-active control systems in numerical studies (Jansen and Dyke 2000, Leitmann 1994, Inaudi 1997, Terasawa and Sano 2005, Bhardwaj and Datta 2006), such as the clipped-optimal and the decentralized bang-bang control algorithms, the linear quadratic Gaussian (LQG),  $H_2$  algorithms etc.. This paper focuses on another control strategy, model predictive control (MPC) scheme, which is based on a prediction model of the system response to obtain the optimal control actions by minimizing an objective function, the prescribed optimization objective is determined by minimizing the difference between the predicted and target responses. For the entire control progress, time delay is one big problem which needs a serious attention, and various methodologies to deal with it have been proposed (Yang *et al.* 1990, Agrawal and Yang 1997, 2000, Chu and Soong 2002, Inaudi and Kelly 1994, Cai and Huang 2002, Kevin 2005a, b, Xu and Li 2008). And the MPC scheme has a function of self-compensation for time delay that occurred in real application.

A kind of MR damper, named MRF-04K damper, had been developed and manufactured, and its dynamic performance had been experimentally studied (Li and Xu 2005). The maximum force at a full magnetic field strength is about 20 kN while the maximum power required is less than 50w. As a numerical example, a 5-story frame structure equipped with 2 MRF-04K dampers is analyzed to demonstrate the validity of the MPC scheme, which exhibits good control performance similar to the LQG control scheme, and shows more effectiveness and robustness for addressing time delay and reducing the structural responses under different earthquakes.

## 2. Predictive control scheme

An  $n$ -degree of freedom building with  $r$  control devices subjected to seismic excitation  $\ddot{u}_g(t)$ , the discrete equation of motion is written as

$$\mathbf{z}(k+1) = \mathbf{G}\mathbf{z}(k) + \mathbf{H}\mathbf{u}(k-d) + \mathbf{W}_1\ddot{u}_g(k) \quad (1)$$

where  $\mathbf{z}(k)$  =  $2n$ -dimensional state vector,  $\mathbf{u}(k-d)$  = a  $r$ -dimensional control action vector, in which  $d\Delta t$ , ( $d = 1, 2, \dots$ ), is the time delay and  $\Delta t$  = sampling period,  $\ddot{u}_g(k)$  = external excitation,  $\mathbf{G} = 2n \times 2n$  state matrix,  $\mathbf{H} = 2n \times r$  matrix, and  $\mathbf{W}_1$  = a  $2n$ -dimensional vector.

Referring to the Eq. (1), the predictive model is defined as

$$\hat{\mathbf{z}}(k+j|k) = \mathbf{G}\hat{\mathbf{z}}(k+j-1|k) + \mathbf{H}\hat{\mathbf{u}}(k+j-1-d|k) \quad (2)$$

$$(j = 1, 2, \dots, l+d)$$

where  $\hat{\mathbf{z}}(k+j|k)$  = a  $2n$ -dimensional state vector at a future sampling period,  $k+j$ , estimated by the information available at time step  $k$ ,  $\hat{\mathbf{u}}(k+j-1-d|k)$  = a  $r$ -dimensional predictive control vector,  $l$  = predictive length. This model can be auto-updated at the  $k$ th time step, that is

$$\hat{\mathbf{z}}(k|k) = \mathbf{z}(k); \quad \hat{\mathbf{u}}(k-j|k) = \mathbf{u}(k-j) \quad (j = 1, 2, \dots, d) \quad (3)$$

Substituting Eq. (3) into (2), the predicted state at the subsequent time steps of  $k+j$ ,  $j = 1, 2, \dots, l+d$ , can be expressed as a function of the current state vector  $\mathbf{z}(k)$  and the control force vector

$\mathbf{u}(k)$ . The last predictive equation,  $j = l + d$ , can be written as follows

$$\begin{aligned} \hat{\mathbf{z}}(k+d+l|k) &= \mathbf{G}^{d+l}\mathbf{z}(k) + \mathbf{G}^{d+l-1}\mathbf{H}\mathbf{u}(k-d) + \dots + \mathbf{G}^l\mathbf{H}\mathbf{u}(k-1) + \\ &\quad \mathbf{G}^{l-1}\mathbf{H}\hat{\mathbf{u}}(k|k) + \mathbf{G}^{l-2}\mathbf{H}\hat{\mathbf{u}}(k+1|k) + \dots + \mathbf{H}\hat{\mathbf{u}}(k+l-1|k) \end{aligned} \quad (4)$$

Assuming that control action is uniform over the duration of predictive period of time, that is

$$\hat{\mathbf{u}}(k|k) = \hat{\mathbf{u}}(k+1|k) = \dots = \hat{\mathbf{u}}(k+l-1|k) \quad (5)$$

The following objective function is selected as

$$J_k = \frac{1}{2}\hat{\mathbf{z}}(k+d+l|k)^T\mathbf{Q}\hat{\mathbf{z}}(k+d+l|k) + \frac{1}{2}\hat{\mathbf{u}}(k|k)^T\mathbf{R}\hat{\mathbf{u}}(k|k) \quad (6)$$

where  $\mathbf{Q}$  and  $\mathbf{R} = 2n \times 2n$  and  $r \times r$  weighting matrices, respectively. Substituting Eq. (5) into Eq. (4)

$$\hat{\mathbf{z}}(k+d+l|k) = \mathbf{G}_1^*\mathbf{z}(k) + \mathbf{H}_1^*\mathbf{U}_k + \mathbf{H}_2^*\hat{\mathbf{u}}(k|k) \quad (7)$$

in which

$$\begin{aligned} \mathbf{G}_1^* &= \mathbf{G}^{d+l} \\ \mathbf{H}_1^* &= [\mathbf{G}^l\mathbf{H}\mathbf{G}^{l+1}\mathbf{H}\dots\mathbf{G}^{d+l-2}\mathbf{H}\mathbf{G}^{d+l-1}\mathbf{H}] \\ \mathbf{H}_2^* &= \mathbf{G}^{l-1}\mathbf{H} + \mathbf{G}^{l-2}\mathbf{H} + \dots + \mathbf{G}\mathbf{H} + \mathbf{H} \\ \mathbf{U}_k &= [\mathbf{u}(k-1)^T, \mathbf{u}(k-2)^T, \dots, \mathbf{u}(k-d)^T]^T \end{aligned} \quad (8)$$

By differentiating  $J_k$  with respect to  $\hat{\mathbf{u}}(k|k)$ ,  $\partial J_k / \partial \hat{\mathbf{u}}(k|k) = 0$ , the optimal predictive control force is given by

$$\mathbf{u}(k) = \hat{\mathbf{u}}(k|k) = -\mathbf{D}_1^*\mathbf{z}(k) - \mathbf{D}_2^*\mathbf{U}_k \quad (9)$$

in which

$$\begin{aligned} \mathbf{D}_1^* &= (\mathbf{H}_2^{*T}\mathbf{Q}\mathbf{H}_2^* + \mathbf{R})^{-1}\mathbf{H}_2^{*T}\mathbf{Q}\mathbf{G}_1^* \\ \mathbf{D}_2^* &= (\mathbf{H}_2^{*T}\mathbf{Q}\mathbf{H}_2^* + \mathbf{R})^{-1}\mathbf{H}_2^{*T}\mathbf{Q}\mathbf{H}_1^* \end{aligned} \quad (10)$$

The prediction of future multi-step state  $\hat{\mathbf{z}}(k+d+l|k)$  is based both on actual past control action  $\mathbf{u}(k)$ ,  $\mathbf{u}(k-1)$ , ...,  $\mathbf{u}(k-d)$  and on actual current measuring response state  $\mathbf{z}(k)$  to reach a prescribed optimization objective that minimizing the difference between the predicted and target responses. The control command determined by the prediction model are then applied to the structure, the next step actual state will be measured, and results of comparison with the predicted one are utilized to update future predictions.

### 3. LQG control scheme

The linear quadratic Gaussian (LQG) control strategy, only requiring accelerations as the feedback, is summarized briefly. The controlled structure is actuated by the external disturbance  $w$  and the control action  $\mathbf{u}$  produced by the controller according to the measurement signal as follows

$$\mathbf{y}_v(t) = \mathbf{y}(t) + \mathbf{v}(t) \quad (11)$$

where  $\mathbf{v}(t)$  = the measurement noise vector, and  $\mathbf{y}(t)$  = the output acceleration vector

$$\mathbf{y}(t) = \mathbf{C}_a \mathbf{z}(t) + \mathbf{D}_a \mathbf{u}(t) + \mathbf{W}_a \ddot{u}_g(t) \quad (12)$$

where

$$\mathbf{C}_a = [-\mathbf{M}^{-1} \mathbf{K} - \mathbf{M}^{-1} \mathbf{C}] \quad \mathbf{D}_a = \mathbf{M}^{-1} \mathbf{E} \quad \mathbf{W}_a = \mathbf{M}^{-1} \mathbf{F} \quad (13)$$

where  $\mathbf{M}$ ,  $\mathbf{K}$  and  $\mathbf{C} = n \times n$  mass, stiffness and damping matrices, respectively,  $\mathbf{E} = n \times r$  location matrix of controllers, and  $\mathbf{F}$  = a  $n$ -dimensional vector denoting the location of excitation.

The LQG control scheme is to devise a control law with constant gain (André 1997)

$$\mathbf{u}(t) = -\mathbf{G}\mathbf{z}(t) = -\mathbf{R}^{-1} \mathbf{B}^T \mathbf{P}\mathbf{z}(t) \quad (14)$$

by minimizing the following quadratic cost function

$$J = \frac{1}{2} \lim_{T \rightarrow \infty} E \left\{ \int_0^T (\mathbf{z}^T(t) \mathbf{Q} \mathbf{z}(t) + \mathbf{u}^T(t) \mathbf{R} \mathbf{u}(t)) dt \right\} \quad (15)$$

where  $\mathbf{P}$  = the symmetric positive definite solution of the algebraic Riccati equation

$$\mathbf{P}\mathbf{A} + \mathbf{A}^T \mathbf{P} + \mathbf{Q} - \mathbf{P}\mathbf{B}\mathbf{R}^{-1} \mathbf{B}^T \mathbf{P} = \mathbf{0} \quad (16)$$

where  $\mathbf{A} = 2n \times 2n$  system matrix, and  $\mathbf{B} = 2n \times r$  input matrix.

From Eq. (14), the control forces can not be derived without full state measurements, however, a state estimate  $\hat{\mathbf{z}}$  can be derived such that  $\mathbf{u}(t) = -\mathbf{G}\hat{\mathbf{z}}(t)$  remains optimal based on the measurements of accelerations. This state estimate is generated by the Kalman filter

$$\begin{aligned} \dot{\hat{\mathbf{z}}}(t) &= \mathbf{A}\hat{\mathbf{z}}(t) + \mathbf{B}\mathbf{u}(t) + \mathbf{L}(\mathbf{y}_v(t) - \mathbf{C}_a \hat{\mathbf{z}}(t) - \mathbf{D}_a \mathbf{u}(t)) \\ &= (\mathbf{A} - \mathbf{L}\mathbf{C}_a) \hat{\mathbf{z}}(t) + (\mathbf{B} - \mathbf{L}\mathbf{D}_a) \mathbf{u}(t) + \mathbf{L}\mathbf{y}_v(t) \end{aligned} \quad (17)$$

in which the filter gain  $\mathbf{L}$  is

$$\mathbf{L} = \mathbf{P}_1 \mathbf{C}_a^T \mathbf{V}^{-1} \quad (18)$$

where  $\mathbf{P}_1$  = a solution of the filter Riccati algebraic equation

$$\mathbf{A}\mathbf{P}_1 + \mathbf{P}_1 \mathbf{A}^T + \mathbf{W}\mathbf{W}_1 \mathbf{W}^T - \mathbf{P}_1 \mathbf{C}_a^T \mathbf{V}^{-1} \mathbf{C}_a \mathbf{P}_1 = \mathbf{0} \quad (19)$$

where  $\mathbf{W}_1$  and  $\mathbf{V}$  = covariance matrices of the noise  $w$  and  $\mathbf{v}$ , respectively.

The full state-space equation of LQG control strategy is as follows

$$\begin{aligned} \dot{\hat{\mathbf{z}}}(t) &= (\mathbf{A} - \mathbf{L}\mathbf{C}_a) \hat{\mathbf{z}}(t) + (\mathbf{B} - \mathbf{L}\mathbf{D}_a) \mathbf{u}(t) + \mathbf{L}\mathbf{y}_v(t) \\ \mathbf{u}(t) &= -\mathbf{G}\hat{\mathbf{z}}(t) \end{aligned} \quad (20)$$

#### 4. MRF-04K damper

A double-ended, shear mode combined with valve mode MRF-04K damper has been designed and manufactured, Fig. 1 shows the picture of this damper, which has an inside diameter of 12.5 cm and a stroke of  $\pm 4$  cm, approximately 0.5 m long and with a mass of 50 kg. The maximum force at

a full magnetic field strength is 21.25 kN at a piston velocity of 12.57 cm/sec (Li and Xu 2005).

The MRF-04K damper is used as semi-active control device and employed in the control system, and a simple Bouc-wen model (Spencer *et al.* 1997b) is used to portray the behavior of this damper, as shown in Fig. 2. The equation governing the force produced by the damper is

$$F = c_0\dot{x} + k_0(x - x_0) + \alpha z \tag{21}$$

and the Bouc-Wen element is

$$\dot{z} = -\gamma|\dot{x}|z|z|^{n-1} - \beta\dot{x}|z|^n + A\dot{x} \tag{22}$$

where  $x$  and  $F(t)$  are the displacement and force of the damper, respectively,  $x_0$  is the initial displacement of spring  $k_0$ , and  $z(t)$  is the evolutionary variable that accounts for the hysteretic behavior of the device, the parameters  $c_0$  and  $\alpha$  are future functions of applied voltage  $u$

$$\begin{aligned} c_0 &= c_{0a} + c_{0b}u \\ \alpha &= \alpha_a + \alpha_b u \end{aligned} \tag{23}$$

The parameters of Bouc-Wen model are selected as follows,  $c_{0a} = 80$  N·sec/cm,  $c_{0b} = 15$  N·sec/cm·V,  $k_0 = 10$  N/cm,  $x_0 = 18.6$  cm,  $\alpha_a = 2.1$  kN/cm,  $\alpha_b = 1.7$  kN/cm·V,  $\gamma = 30$  cm<sup>-2</sup>,  $\beta = 30$  cm<sup>-2</sup>,  $n = 2$ , and  $A = 60$ . The typical predicted and experimental responses of the MRF-04K damper due to the 1.0 Hz sinusoidal excitation with amplitude of 10 mm are shown in Fig. 3 for five voltage levels of 0, 2.5, 5.0, 7.5, and 10 V, respectively. The Bouc-Wen model can accurately portray the behavior of the MRF-04K damper.

The control force  $F(t)$  produced by the MRF-04K damper can be controlled by adjusting the voltage applied to the current driver connected with the damper, so the simple bang-bang control law is defined as follows

$$V_i(t) = \begin{cases} V_{\max} & \text{while } F_i(t) \cdot u_i(t) > 0 \text{ and } |F_i(t)| < u_i(t) \\ 0 & \text{other} \end{cases} \tag{24}$$

where  $V_{\max}$  = maximum applied voltage. If the magnitude of the force  $F_i(t)$  produced by the  $i$ th device is smaller than that of the desired optimal force  $u_i(t)$  and the two forces have the same sign, the voltage applied to the  $i$ th damper is increased to the maximum level, otherwise, the commanded voltage is set to zero.

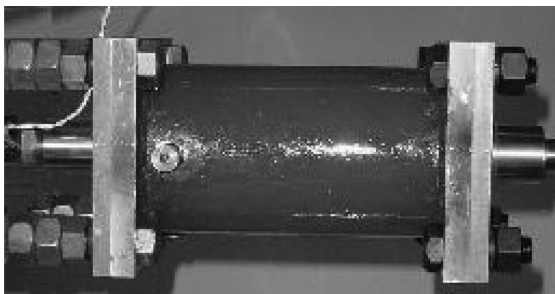


Fig. 1 MRF-04K damper

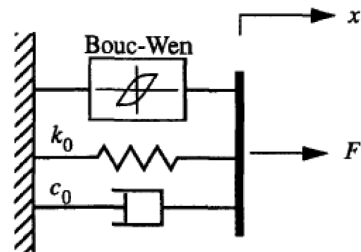


Fig. 2 Bouc-Wen model

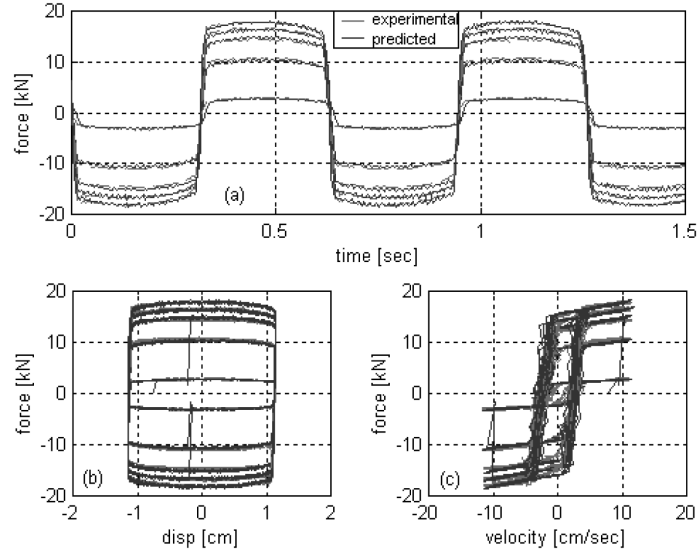


Fig. 3 Experimental and predicted damper force due to 1.0 Hz sinusoidal excitation with amplitude of 10 mm: (a) force versus time, (b) force versus displacement, and (c) force versus velocity

## 5. Numerical example

To evaluate the proposed MPC scheme and LQG scheme for use in semi-active control system with MR dampers, a numerical example is considered in which a 5-story frame structure (Johnson *et al.* 1998) is controlled with MRF-04K dampers, and the structural properties are given in Table 1. According to the structural stiffness properties and the plan collocation, after trial and error calculation to determine the locations of MR dampers. Two MRF-04K dampers are installed in combination with steel braces on the first floor and the third floor, assuming that the steel braces are infinity rigid. Two historical earthquake records, El Centro (1940 NS) and Northridge (1994 NS), are considered, and the peak acceleration of the ground motion is taken as 0.2 g.

The control performance of the MPC scheme with MR dampers declines while the predictive length,  $l$ -value, exceeds a specific value (Xu and Li 2008). In the numerical analysis, the predictive length  $l = 5$  and the delayed time step  $d = 10, 20, 40, 60, 100$  are considered to examine the validity of the MPC scheme for addressing time delay and reducing the structural responses under different earthquakes. For El Centro and Northridge earthquake, the sampling periods are, respectively, 0.02 s and 0.01 s, and the time delay magnitudes ranges, respectively, from 0.2 s to 2.0 s and from 0.1 s to 1.0 s. The results for MPC and LQG scheme are shown in Table 2. Ten criteria ( $J_1 - J_6$  and  $J_{11} - J_{14}$ ) provided by ASCE benchmark control problems (Ohtori *et al.* 2004) are used to evaluate the performance of control scheme, and  $J_1$  to  $J_6$  are related to the building responses,  $J_{11}$  to  $J_{14}$  are related to the control devices. To evaluate the effects of different  $d$ -value on control performance, the following index is defined as

$$J_{im} = \left( 1 - \max_{\substack{\text{EL Centro} \\ \text{Northridge}}} \{J_i\} \right) \times 100\% \quad (i = 1, 2, 4, 5) \quad (25)$$

Table 1 Properties of controlled structure

Story	1	2	3	4	5
Stiffness ( $\times 10^3$ kN/m)	33.732	29.093	28.621	24.954	19.059
Weight (kN)	58.97	58.97	58.97	58.97	58.97
Damping (kNs/m)	67	58	57	50	38

Table 2 Evaluation criteria for SAPC and LQG scheme due to different earthquakes

	El Centro Earthquake						Northridge Earthquake					
	LQG	MPC					LQG	MPC				
		$d=10$	$d=20$	$d=40$	$d=60$	$d=100$		$d=10$	$d=20$	$d=40$	$d=60$	$d=100$
$J_1$	0.786	0.688	0.745	0.782	0.860	0.966	0.588	0.571	0.754	0.753	0.877	0.922
$J_2$	0.985	0.797	0.964	0.999	0.971	1.000	0.792	0.650	0.941	0.666	0.840	0.858
$J_3$	0.937	0.832	0.879	0.936	0.975	1.007	0.609	0.630	0.991	0.742	0.935	0.846
$J_4$	0.635	0.593	0.613	0.724	0.747	0.882	0.541	0.527	0.693	0.667	0.715	0.854
$J_5$	0.668	0.732	0.601	0.753	0.746	0.876	0.544	0.461	0.948	0.585	0.677	0.818
$J_6$	0.641	0.713	0.571	0.812	0.779	0.880	0.507	0.422	0.810	0.545	0.728	0.782
$J_{11}$	2.9E-2	4.2E-2	3.6E-2	5.4E-2	2.8E-2	3.3E-2	4.7E-2	6.0E-2	5.4E-2	5.5E-2	5.1E-2	5.4E-2
$J_{12}$	0.399	0.349	0.378	0.397	0.436	0.490	0.305	0.296	0.391	0.391	0.455	0.479
$J_{13}$	7.8E-6	7.8E-6	7.8E-6	7.8E-6	7.8E-6	7.8E-6	2.7E-6	2.7E-6	2.7E-6	2.7E-6	2.7E-6	2.7E-6
$J_{14}$	3.3E-3	3.5E-3	3.3E-3	3.2E-3	2.7E-3	2.2E-3	4.1E-3	4.3E-3	4.3E-3	4.2E-3	3.7E-3	3.7E-3

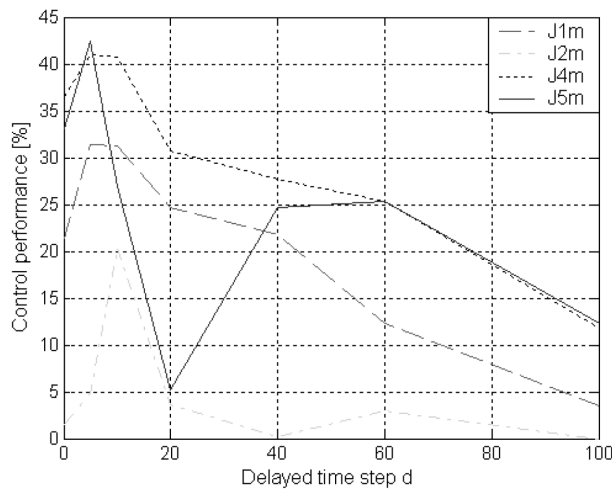


Fig. 4 Effects of different  $d$  value on control performance

Fig. 4 shows the effects of different  $d$ -value on control performance, which also conducts a comparison of LQG scheme without delayed time ( $d=0$ ) with MPC scheme with different delayed time ( $d=10, 20, 40, 60, 100$ ) in semi-active control system using MR dampers. Table 3 and Table 4 show the peak values, and Table 5 and Table 6 show the root mean square (RMS) values, of the

Table 3 Peak responses for passive control, LQG scheme, and MPC scheme due to El Centro earthquakes

Floor No.	No Control		Passive-off		Passive-on		LQG Scheme		MPC ( $l = 5, d = 20$ )	
			$F_{1\max} = 1.61$ kN		$F_{1\max} = 9.62$ kN		$F_{1\max} = 7.85$ kN		$F_{1\max} = 7.82$ kN	
	$x_i$ /mm	$\ddot{x}_i$ /m/s <sup>2</sup>	$x_i$ /mm	$\ddot{x}_i$ /m/s <sup>2</sup>	$x_i$ /mm	$\ddot{x}_i$ /m/s <sup>2</sup>	$x_i$ /mm	$\ddot{x}_i$ /m/s <sup>2</sup>	$x_i$ /mm	$\ddot{x}_i$ /m/s <sup>2</sup>
			$F_{3\max} = 1.65$ kN		$F_{3\max} = 8.77$ kN		$F_{3\max} = 8.50$ kN		$F_{3\max} = 10.42$ kN	
1	4.752	2.850	4.354	2.821	3.113	2.563	3.593	2.860	3.610	2.703
2	9.652	4.321	8.867	4.249	6.583	3.687	7.444	4.378	7.260	3.905
3	13.632	5.477	12.583	5.164	9.409	4.575	10.374	5.256	10.317	4.988
4	16.773	6.600	15.596	6.143	12.059	5.358	12.827	6.174	12.505	5.925
5	18.845	7.710	17.591	7.567	14.025	6.889	14.463	7.593	14.116	7.435

Table 4 Peak responses for passive control, LQG scheme, and MPC scheme due to Northridge earthquakes

Floor No.	No Control		Passive-off		Passive-on		LQG Scheme		MPC ( $l = 5, d = 20$ )	
			$F_{1\max} = 2.05$ kN		$F_{1\max} = 15.2$ kN		$F_{1\max} = 9.44$ kN		$F_{1\max} = 13.4$ kN	
	$x_i$ /mm	$\ddot{x}_i$ /m/s <sup>2</sup>	$x_i$ /mm	$\ddot{x}_i$ /m/s <sup>2</sup>	$x_i$ /mm	$\ddot{x}_i$ /m/s <sup>2</sup>	$x_i$ /mm	$\ddot{x}_i$ /m/s <sup>2</sup>	$x_i$ /mm	$\ddot{x}_i$ /m/s <sup>2</sup>
			$F_{3\max} = 1.98$ kN		$F_{3\max} = 14.3$ kN		$F_{3\max} = 13.44$ kN		$F_{3\max} = 15.7$ kN	
1	6.275	2.884	5.871	2.685	4.165	2.409	3.462	2.639	4.841	5.929
2	13.048	5.254	12.239	4.952	8.834	4.387	7.447	4.877	9.895	4.411
3	18.898	7.132	17.709	6.788	12.513	5.280	11.038	5.546	14.422	10.361
4	23.852	9.333	22.360	8.786	15.749	5.995	14.716	6.711	17.908	7.192
5	27.349	11.025	25.623	10.385	17.894	6.791	17.507	8.735	20.526	8.116

Table 5 RMS responses for passive control, LQG scheme, and MPC scheme due to El Centro earthquakes

Floor No.	No Control		Passive-off		Passive-on		LQG Scheme		MPC ( $l = 5, d = 20$ )	
			$\sigma_{F_1} = 0.60$ kN		$\sigma_{F_1} = 4.39$ kN		$\sigma_{F_1} = 2.13$ kN		$\sigma_{F_1} = 2.15$ kN	
	$\sigma_{x_i}$ /mm	$\sigma_{\ddot{x}_i}$ /m/s <sup>2</sup>	$\sigma_{x_i}$ /mm	$\sigma_{\ddot{x}_i}$ /m/s <sup>2</sup>	$\sigma_{x_i}$ /mm	$\sigma_{\ddot{x}_i}$ /m/s <sup>2</sup>	$\sigma_{x_i}$ /mm	$\sigma_{\ddot{x}_i}$ /m/s <sup>2</sup>	$\sigma_{x_i}$ /mm	$\sigma_{\ddot{x}_i}$ /m/s <sup>2</sup>
			$\sigma_{F_3} = 0.57$ kN		$\sigma_{F_3} = 4.15$ kN		$\sigma_{F_3} = 2.86$ kN		$\sigma_{F_3} = 3.18$ kN	
1	1.552	0.684	1.429	0.637	1.170	0.656	0.968	0.501	0.980	0.635
2	3.209	1.319	2.965	1.231	2.530	1.183	2.018	0.947	1.995	0.852
3	4.620	1.866	4.270	1.728	3.669	1.637	2.897	1.237	2.853	1.176
4	5.797	2.333	5.372	2.172	4.736	2.087	3.673	1.526	3.548	1.384
5	6.619	2.680	6.141	2.501	5.488	2.452	4.218	1.791	4.035	1.609

displacement, acceleration and control force at different floors under different control schemes due to different earthquakes.

It can be noted that the control performance of MPC scheme is declined as the delayed time increases and the changes in required control power are very small. As shown the performance criteria in Table 2 and Fig. 4, the MPC scheme has better control effectiveness than LQG scheme while the delayed time step is less than 20, and similar control effectiveness as LQG scheme while

Table 6 RMS responses for passive control, LQG scheme, and MPC scheme due to Northridge earthquakes

Floor No.	No Control		Passive-off		Passive-on		LQG Scheme		MPC ( $l = 5, d = 20$ )	
			$\sigma_{F_1} = 0.89$ kN		$\sigma_{F_1} = 6.72$ kN		$\sigma_{F_1} = 2.07$ kN		$\sigma_{F_1} = 2.71$ kN	
	$\sigma_{x_i}$ /mm	$\sigma_{\ddot{x}_i}$ /m/s <sup>2</sup>	$\sigma_{F_3} = 0.85$ kN	$\sigma_{F_3} = 6.61$ kN	$\sigma_{F_3} = 3.56$ kN	$\sigma_{F_3} = 5.5$ kN	$\sigma_{x_i}$ /mm	$\sigma_{\ddot{x}_i}$ /m/s <sup>2</sup>	$\sigma_{x_i}$ /mm	$\sigma_{\ddot{x}_i}$ /m/s <sup>2</sup>
1	1.699	0.669	1.510	0.595	1.128	0.555	0.930	0.448	1.237	1.231
2	3.505	1.362	3.132	1.223	2.500	1.166	1.905	0.848	2.486	0.901
3	5.038	1.949	4.502	1.742	3.637	1.635	2.708	1.038	3.551	2.653
4	6.313	2.443	5.663	2.199	4.773	2.142	3.409	1.260	4.325	1.436
5	7.201	2.799	6.471	2.526	5.575	2.543	3.901	1.524	4.863	1.666

the delayed time step is between 20 and 40 for most evaluation criteria under both earthquakes, but the control performance declines sharply while  $d$ -value exceeds 60. When the delayed time reach 2.0 s ( $d = 100$  for El Centro earthquake), the MPC scheme also has some control effectiveness except for the peak acceleration and base shear, which indicate that the MPC scheme has a good performance for addressing time delay. The effect of different  $d$ -value on control performance depends on the input motions and the properties of control devices, for both earthquakes in this paper, the controlled responses will become larger than uncontrolled ones while  $d$ -value exceeds 100.

A performance comparison among passive-off (0 Volts), passive-on (10 Volts), LQG scheme, and MPC scheme ( $d = 20$ ) is also conducted, as shown in Table 3 to Table 6. Comparing with the uncontrolled responses, the controlled ones are all clearly reduced by different control schemes except that the peak and RMS accelerations at the first and the third floor under MPC scheme due to Northridge earthquake. LQG and MPC schemes used in semi-active control system have better control performance than two passive control methods for most cases under different earthquakes, especially for the reduction of the root mean square responses. Even the delayed time reaches 0.4 s for El Centro earthquake, control performance of MPC scheme is better than that of LQG scheme, the peak control force is 10.42 kN under MPC while it is 8.5 kN under LQG scheme, and the RMS control force is 3.18 kN under MPC while it is 2.86 kN under LQG scheme. For both earthquake inputs, the RMS control forces produced by MRF-04K damper are less than the passive-on method, as shown in Table 5 and Table 6. The controlled peak acceleration at the top floor under MPC scheme is 7.44 m/s<sup>2</sup> and 8.12 m/s<sup>2</sup>, respectively, for El Centro and Northridge earthquakes, which is similar to that of LQG scheme, 7.60 m/s<sup>2</sup> and 8.74 m/s<sup>2</sup>, as listed in Table 3 and Table 4.

From the numerical examples, MPC scheme exhibits good control performance similar to the LQG control scheme even the delayed time reaches 0.4 s. MPC scheme is based on a prediction model of the system response to obtain the optimal control actions by minimizing an object function, which can predict the next multi-step responses of structure according to the current states, and compensate for delayed time that occurred in real application. MPC scheme used in semi-active control system with MR dampers show more effectiveness and robustness for addressing time delay, when the delayed time reaches 2.0 s, which also has some control effectiveness.

## 6. Conclusions

A model predictive control (MPC) strategy is proposed and employed in semi-active control system with MR dampers to reduce structural responses under different earthquake excitations. The MPC scheme is based on a prediction model of the system response to obtain the control actions by minimizing an objective function, the prescribed optimization objective is determined by minimizing the difference between the predicted and target responses, which has a function of self-compensation for time delay that occurred in real application. As a numerical example, a 5-story building equipped with two 20 kN MRF-04K dampers is introduced to demonstrate the validity of this approach. Comparison with passive-off, passive-on, and LQG scheme indicates that MPC scheme exhibits good control performance similar to the LQG control scheme even the delayed time reaches 0.4 s, both have better control effectiveness than two passive control methods for most cases under different earthquakes, especially for the reduction of the root mean square responses, and the MPC scheme used in semi-active control system show more effectiveness and robustness for addressing time delay, when the delayed time reaches 2.0 s, it also has some control effectiveness.

## Acknowledgements

The writers gratefully acknowledge the partial support of this research by the National Natural Science Foundation of China under Grant No. 90815025 and 90715032, and 50808013, and 51178034, and the Fundamental Research Funds for the Central Universities under Grant No. 2011JBM258.

## References

- Agrawal, A.K. and Yang, J.N. (1997), "Effect of fixed time-delay on stability and performance of actively controlled civil engineering structures", *Earthq. Eng. Struct. D.*, **26**(11), 1169-1185.
- Agrawal, A.K. and Yang, J.N. (2000), "Compensation of time-delay for control of civil engineering structures", *Earthq. Eng. Struct. D.*, **29**, 37-62.
- André, P. (1997), *Vibration Control of Active Structures*, Kluwer Academic Publishers, Boston.
- Bhardwaj, M.K. and Datta, T.K. (2006), "Semiactive fuzzy control of the seismic response of building frames", *J. Struct. Eng.-ASCE*, **132**(5), 791-799.
- Cai, G.P. and Huang, J.Z. (2002), "Optimal control method for seismically excited building structures with time-delay in control", *J. Eng. Mech.-ASCE*, **128**(6), 602-612.
- Carlson, J.D. and Spencer, Jr. B.F. (1996a), "Magneto-rheological fluid dampers for semi-active seismic control", *Proceedings of 3rd International Conference on Motion and Vibration Control*, China, Japan.
- Carlson, J.D. and Spencer, Jr. B.F. (1996b), "Magneto-rheological fluid dampers: scalability and design issues for application to dynamic hazard mitigation", *Proceedings of 2nd International Workshop on Structural Control*, Hong Kong.
- Chang, C.C. and Roschke, P.N. (1999), "Neural network modeling of a magnetorheological damper", *J. Intell. Mater. Syst. Struct.*, **9**(9), 755-764.
- Chu, S.Y., Soong, T.T., Lin, C.C. and Chen, Y.Z. (2002), "Time-delay effect and compensation on direct output feedback controlled mass damper systems", *Earthq. Eng. Struct. D.*, **31**(1), 121-137.
- Dyke, S.J., Spencer, Jr. B.F., Sain, M.K. and Carlson, J.D. (1996), "Seismic response reduction using

- magnetorheological dampers”, *Proceedings of IFAC World Congress*, San Francisco, CA, June-July.
- Hiemenz, G.J., Choi, Y.T. and Wereley, N.M. (2003), “Seismic control of civil structures utilizing semi-active MR braces”, *Comput. Aid. Civil Inf.*, **18**(1), 31-44.
- Inaudi, J.A. and Kelly, J.M. (1994), “A robust delay-compensation technique based on memory”, *Earthq. Eng. Struct. D.*, **23**(9), 987-1001.
- Inaudi, J.A. (1997), “Modulated homogeneous friction: a semi-active damping strategy”, *Earthq. Eng. Struct. D.*, **26**(3), 361-376.
- Jansen, L.M. and Dyke, S.J. (2000), “Semi-active control strategies for MR dampers: comparative study”, *J. Eng. Mech.-ASCE*, **126**(8), 795-803.
- Johnson, E.A., Ramallo, J.C., Spencer, Jr. B.F. and Sain, M.K. (1998), “Intelligent base isolation systems”, *Proceedings of the Second World Conference on Structural Control*, Kyoto, Japan, June-July.
- Kevin, K.F. Wong (2005a), “Predictive optimal linear control of elastic structures during earthquake. part I”, *J. Eng. Mech.-ASCE*, **131**(2), 131-141.
- Kevin, K.F. Wong (2005b), “Predictive optimal linear control of inelastic structures during earthquake. part II”, *J. Eng. Mech.-ASCE*, **131**(2), 142-152.
- Leitmann, G. (1994), “Semiactive control for vibration attenuation”, *J. Intell. Mater. Syst. Struct.*, **5**(6), 841-846.
- Li, Z.X. and Xu, L.H. (2005), “Performance tests and hysteresis model of MRF-04K damper”, *J. Struct. Eng.-ASCE*, **131**(8), 1303-1306.
- Ohtori, Y., Christenson, R.E., Spencer, Jr. B.F. and Dyke, S.J. (2004), “Benchmark control problems for seismically excited nonlinear buildings”, *J. Eng. Mech.-ASCE*, **130**(4), 366-385.
- Schurter, K.C. and Roschke, P.N. (2000), “Fuzzy modeling of a magnetorheological damper using ANFIS”, *Proceedings of the ninth IEEE International Conference on Fuzzy Systems*, **1**, 122-127.
- Spencer, Jr. B.F., Carlson, J.D., Sain, M.K. and Yang, G. (1997a), “On the current status of magnetorheological dampers: seismic protection of full-scale structures”, *Proceedings of American Control Conference*, Albuquerque, New Mexico.
- Spencer, Jr. B.F., Dyke, S.J., Sain, M.K. and Carlson, J.D. (1997b), “Phenomenological model for magnetorheological dampers”, *J. Struct. Eng.-ASCE*, **123**(3), 230-238.
- Terasawa, T. and Sano, A. (2005), “Fully adaptive vibration control for uncertain structure installed with MR damper”, *Proceedings of the American Control Conference*, **7**, 4753-4759.
- Xu, L.H. and Li, Z.X. (2008), “Semi-active multi-step predictive control of structures using MR dampers”, *Earthq. Eng. Struct. D.*, **37**, 1435-1448.
- Yang, J.N., Akbarpour, A. and Askar, G. (1990), “Effect of time delay on control of seismic-excited buildings”, *J. Struct. Eng.-ASCE*, **116**(10), 2801-2814.
- Yang, G., Spencer, Jr. B.F., Jung, H.J. and Carlson, J.D. (2004), “Dynamic modeling of large-scale magnetorheological damper systems for civil engineering applications”, *J. Eng. Mech.-ASCE*, **139**(9), 1107-1114.